

SUPPORTING INFORMATION

2D-Coordination Polymers based on 1H-Indazole-4-carboxylic acid and Transition Metal ions: Magnetic, Luminescent and Biological Properties

Antonio A. García-Valdivia,^a Andoni Zabala-Lekuona,^b Gloria B. Ramírez-Rodríguez,^a José M. Delgado-López,^a Belén Fernández,^c Javier Cepeda,^b and Antonio Rodríguez-Díéguez ^{a,*}

Index:

- 1. Crystallographic Tables**
- 2. Continuous Shape Measurements.**
- 3. Figures of supramolecular structures.**
- 4. Magnetic measurements**
- 5. Infrared Spectra**

Table S1.- Bond lengths (Å) and angles (°) for compounds **1** and **2**. Symmetry operations: (i) – x, -y, -z; (ii) –x, -y+1, -z+1.

Compound	1	2	
Co1-O1	2.091(1)	Ni1-O1	2.066(1)
Co1-O1(i)	2.091(1)	Ni 1-O1(ii)	2.066(1)
Co1-O1W	2.126(1)	Ni 1-O1W	2.096(1)
Co1-O1W(i)	2.126(1)	Ni 1-O1W(ii)	2.096(1)
Co1-N1	2.154(1)	Ni 1-N1	2.097(1)
Co1-N1(i)	2.154(1)	Ni 1-N1(ii)	2.097(1)
O1-Co1-O1(i)	180.0	O1-Ni1-O1(I)	180.0
O1-Co1-O1W	90.93(3)	O1-Ni1-O1W	92.02(3)
O1(i)-Co1-O1W	89.07(3)	O1(I)-Ni1-O1W	87.98(3)
O1-Co1-O1W(I)	89.06(3)	O1-Ni1-O1W(I)	87.98(3)
O1(i)-Co1-O1W(i)	90.94(3)	O1(I)-Ni1-O1W(I)	92.02(3)
O1W-Co1-O1W(i)	180.0	O1W-Ni1-O1W(I)	180.0
O1-Co1-N1	87.76(4)	O1-Ni1-N1	92.57(4)
O1(i)-Co1-N1	92.24(4)	O1(I)-Ni1-N1	87.43(4)
O1W-Co1-N1	90.05(4)	O1W-Ni1-N1	89.48(4)
O1W(I)-Co1-N1	89.95(4)	O1W(I)-Ni1-N1	90.52(4)
O1-Co1-N1(i)	92.24(4)	O1-Ni1-N1(I)	87.43(4)
O1(i)-Co1-N1(i)	87.76(4)	O1(I)-Ni1-N1(I)	92.57(4)
O1W-Co1-N1(i)	89.95(4)	O1W-Ni1-N1(I)	90.52(4)
O1W(I)-Co1-N1(i)	90.05(4)	O1W(I)-Ni1-N1(I)	89.48(4)
N1-Co1-N1(i)	180.0	N1-Ni1-N1(I)	180.00(3)

Table S2.- Bond lengths (Å) and angles (°) for compound **3**.

Compound	3
Cu1-O1A	1.947(3)
Cu1-O1B	1.972(3)
Cu1-O1W	2.362(4)
Cu1-N1A	2.014(4)
Cu1-N1B	1.993(4)
O1A-Cu1-O1B	175.82(15)
O1A-Cu1-N1B	89.45(16)
O1B-Cu1-N1B	91.26(15)
O1A-Cu1-N1A	90.98(15)
O1B-Cu1-N1A	87.75(15)
N1B-Cu1-N1A	172.18(18)
O1A-Cu1-O1W	87.63(13)
O1B-Cu1-O1W	96.35(14)
N1B-Cu1-O1W	98.14(15)
N1A-Cu1-O1W	89.68(15)

Table S3.- Bond lengths (\AA) and angles ($^\circ$) for compound **5**. Symmetry operations: (i) $-x+1$, $y+1/2$, $-z+1/2$; (ii) $x+1/2$, $-y+1$, $-z+1/2$; (iii) $-x+3/2$, $-y+3/2$, z .

Compound	5
Cd1-N1(i)	2.267(10)
Cd1-N1(ii)	2.267(10)
Cd1-O1	2.291(9)
Cd1-O1(iii)	2.291(9)
Cd1-O2	2.448(9)
Cd1-O2(iii)	2.448(10)
N1(i)-Cd1-N1(ii)	110.5(5)
N1(i)-Cd1-O1	100.5(3)
N1(ii)-Cd1-O1	97.5(3)
N1(i)-Cd1-O1(iii)	97.5(3)
N1(ii)-Cd1-O1(iii)	100.5(3)
O1-Cd1-O1(iii)	148.3(5)
N1(i)-Cd1-O2(iii)	149.2(3)
N1(ii)-Cd1-O2(iii)	90.6(3)
O1-Cd1-O2(iii)	98.7(3)
O1(iii)-Cd1-O2(iii)	55.4(3)
N1(i)-Cd1-O2	90.6(3)
N1(ii)-Cd1-O2	149.2(3)
O1-Cd1-O2	55.4(3)
O1(iii)-Cd1-O2	98.7(3)
O2(iii)-Cd1-O2	80.7(4)

2. Continuous Shape Measurements

The nearer the value to zero, the better fits to an ideal polyhedron.

Table S4.- Continuous Shape Measurements for compounds **1, 2 and 5**.

HP-6	1 D6h Hexagon
PPY-6	2 C5v Pentagonal pyramid
OC-6	3 Oh Octahedron
TPR-6	4 D3h Trigonal prism
JPPY-6	5 C5v Johnson pentagonal pyramid J2

Structure [ML6]	HP-6	PPY-6	OC-6	TPR-6	JPPY-6
Comp1 Co1	32.146	29.617	0.044	16.397	32.961
Comp2 Ni1	31.775	29.505	0.060	16.186	32.854
Comp5 Cd1	29.641	20.397	5.963	12.968	25.099

Table S5.- Continuous Shape Measurements for compound **3**.

PP-5	1 D5h Pentagon
vOC-5	2 C4v Vacant octahedron
TBPY-5	3 D3h Trigonal bipyramidal
SPY-5	4 C4v Spherical square pyramid
JTBPY-5	5 D3h Johnson trigonal bipyramidal J12

Structure [ML5]	PP-5	vOC-5	TBPY-5	SPY-5	JTBPY-5
Comp3 Cu1	30.052	0.945	5.690	0.832	8.668

Table S6.- Continuous Shape Measurements for compound **5** considering CdN₂C₂ coordination environment.

SP-4	1 D4h Square
T-4	2 Td Tetrahedron
SS-4	3 C2v Seesaw
vTBPY-4	4 C3v Vacant trigonal bipyramidal

Structure [ML4]	SP-4	T-4	SS-4	vTBPY-4
Comp5 Cd1	22.557	2.297	6.480	4.881

3. Figures of supramolecular structures

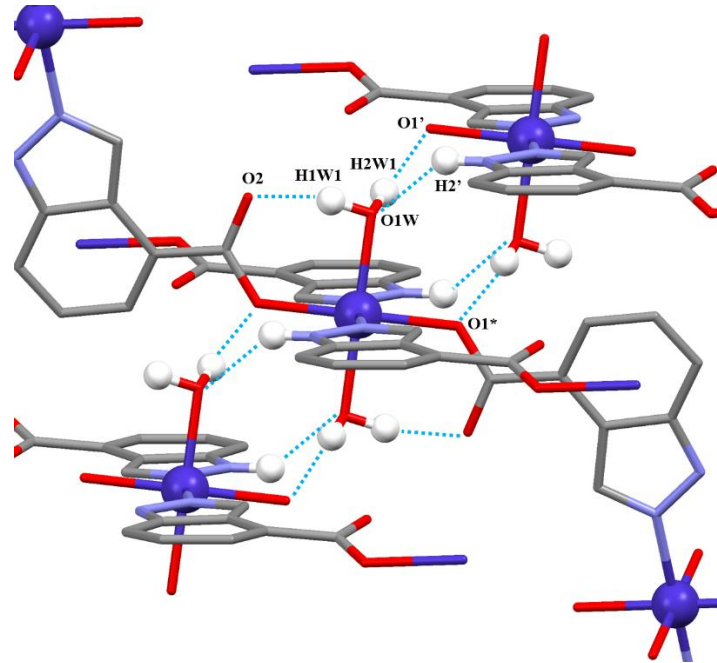


Figure S1.- Intra- and intermolecular hydrogen bonds that stabilize the supramolecular structure of compound **1**.

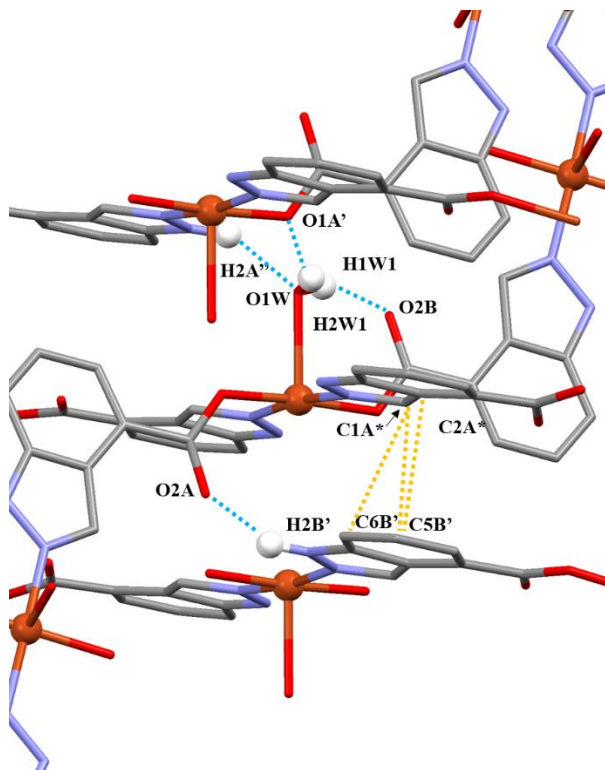


Figure S2.- Intra- and intermolecular hydrogen bonds (dashed blue lines) as well as intermolecular π···π interactions (dashed yellow lines) that stabilize the supramolecular structure of compound **3**.

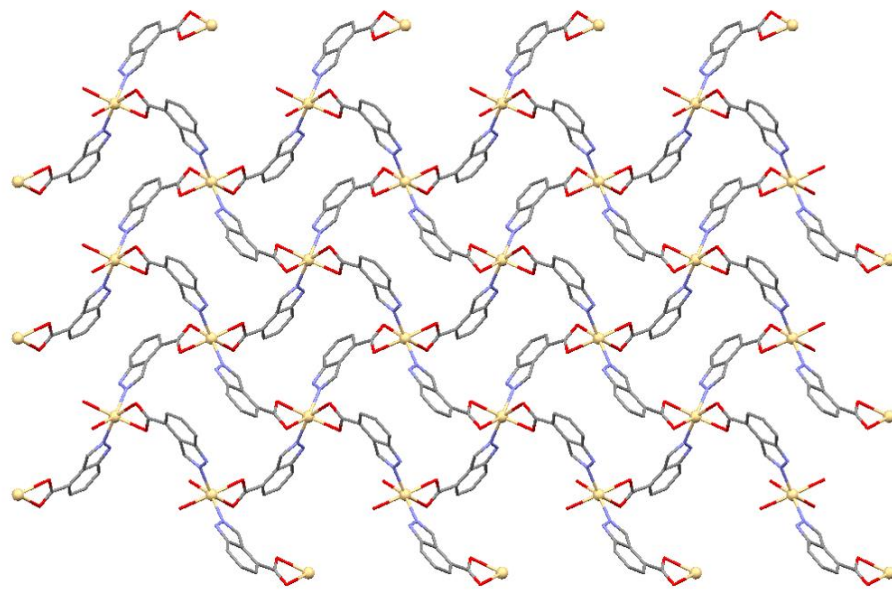


Figure S3.- Perspective view of a 2D layer of compound **5** in the *ab* plane.

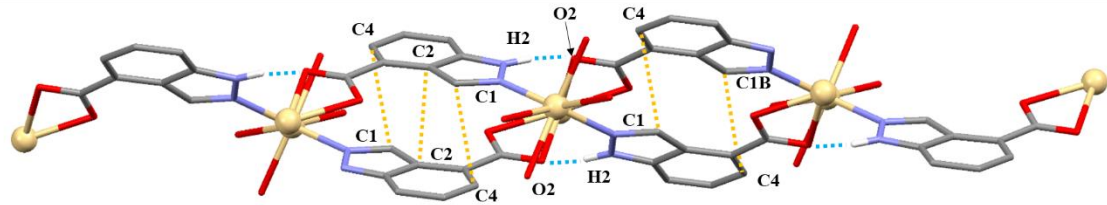


Figure S4.- Intermolecular hydrogen bonds (dashed blue lines) and $\pi \cdots \pi$ interactions (dashed yellow lines) that are responsible of the packing structure of the 2D layers in compound **5**.

4. Magnetic measurements

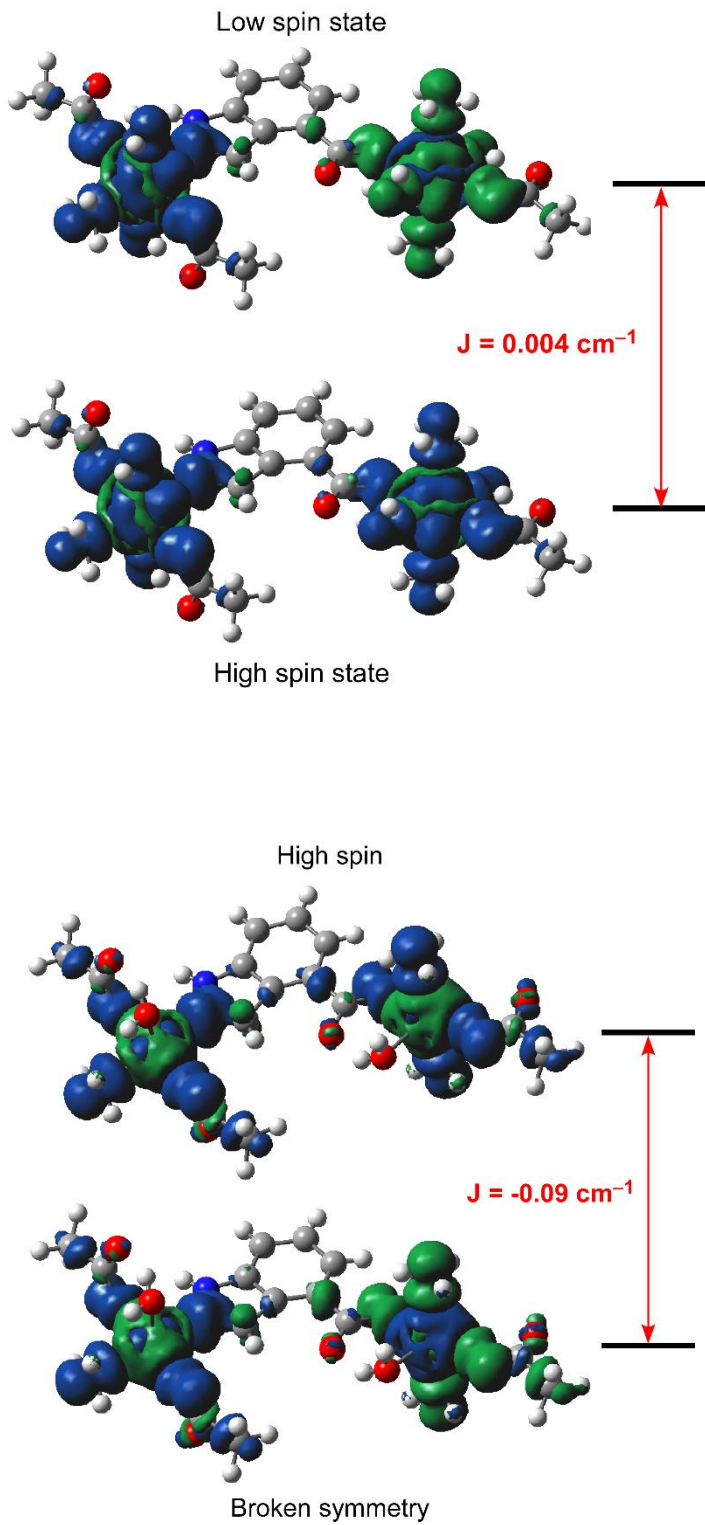


Figure S5.- Broken-symmetry DFT based calculation on **1** (top) and **3** (down) to account for the value of the exchange parameter. Spin densities are shown for ground and excited states involving the superexchange pathway.

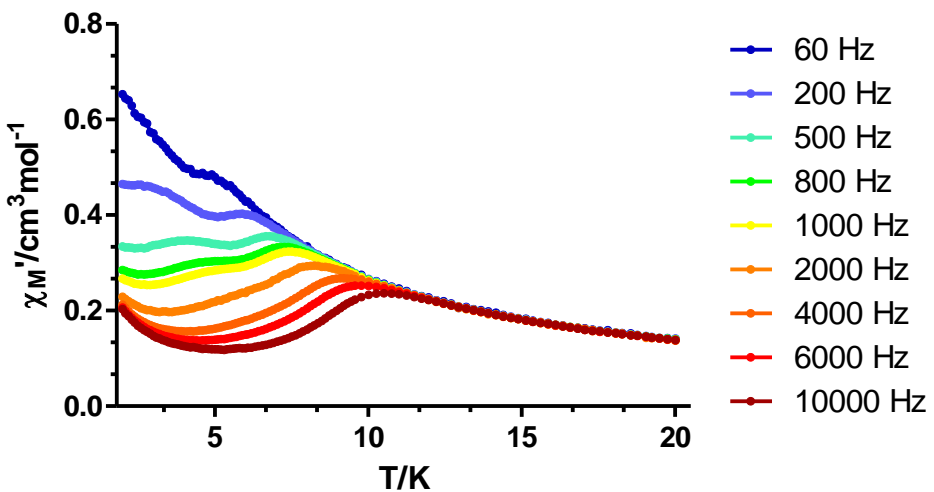


Figure S6.- Temperature dependence of in-phase components of the *ac* susceptibility in a *dc* applied field of 1000 Oe for **1**.

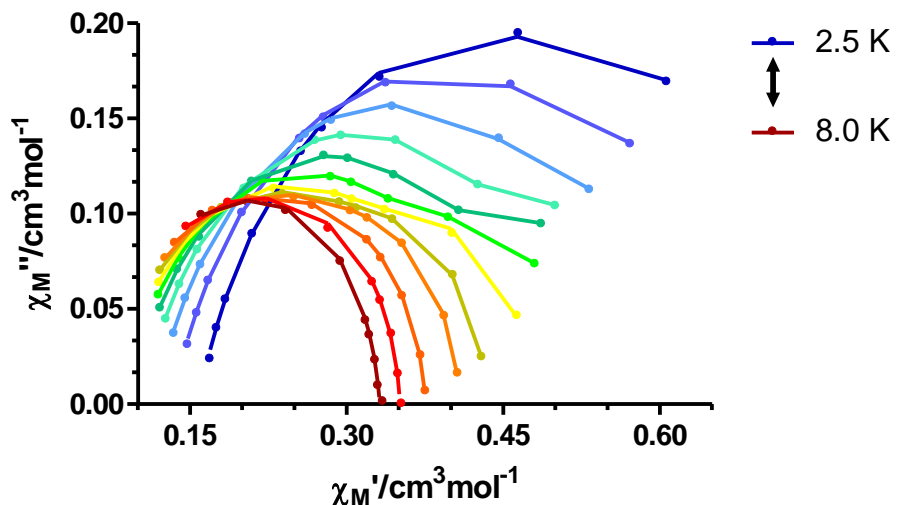


Figure S7.- Cole-Cole plots in a *dc* applied field of 1000 Oe for **1**. Solid lines represent the best fitting of the experimental data to the Debye model.

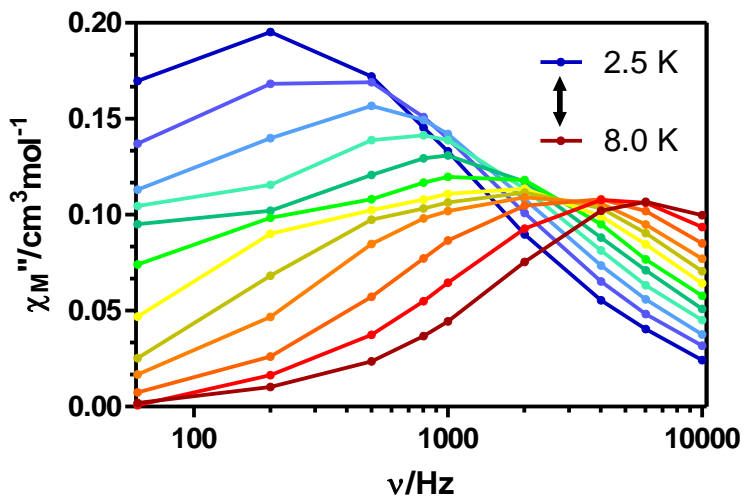


Figure S8.- Variable-temperature frequency dependence of the χ_M'' signal under 1000 Oe applied field for **1**. Solid lines are a guide to the eye.

Table S7. Relaxation Fitting Parameters from Least-Squares Fitting of $\chi(\phi)$ data for complex **1**.

T (K)	FR		SR	
	α_1	τ_1	α_2	τ_2
2.5	0.22	5.62E-04	-	-
3.0	0.23	4.09E-04	-	-
3.5	0.22	2.94E-04	-	-
4.0	0.22	2.04E-04	-	-
4.5	0.21	1.44E-04	-	-
5.0	0.20	1.03E-04	-	-
5.5	0.19	7.51E-05	-	-
6.0	-	-	~0.00	4.30E-04
6.5	-	-	~0.00	2.67E-04
7.0	-	-	~0.00	1.38E-04
7.5	-	-	~0.00	7.82E-05
8.0	-	-	~0.00	4.06E-05

5. Infrared Spectra

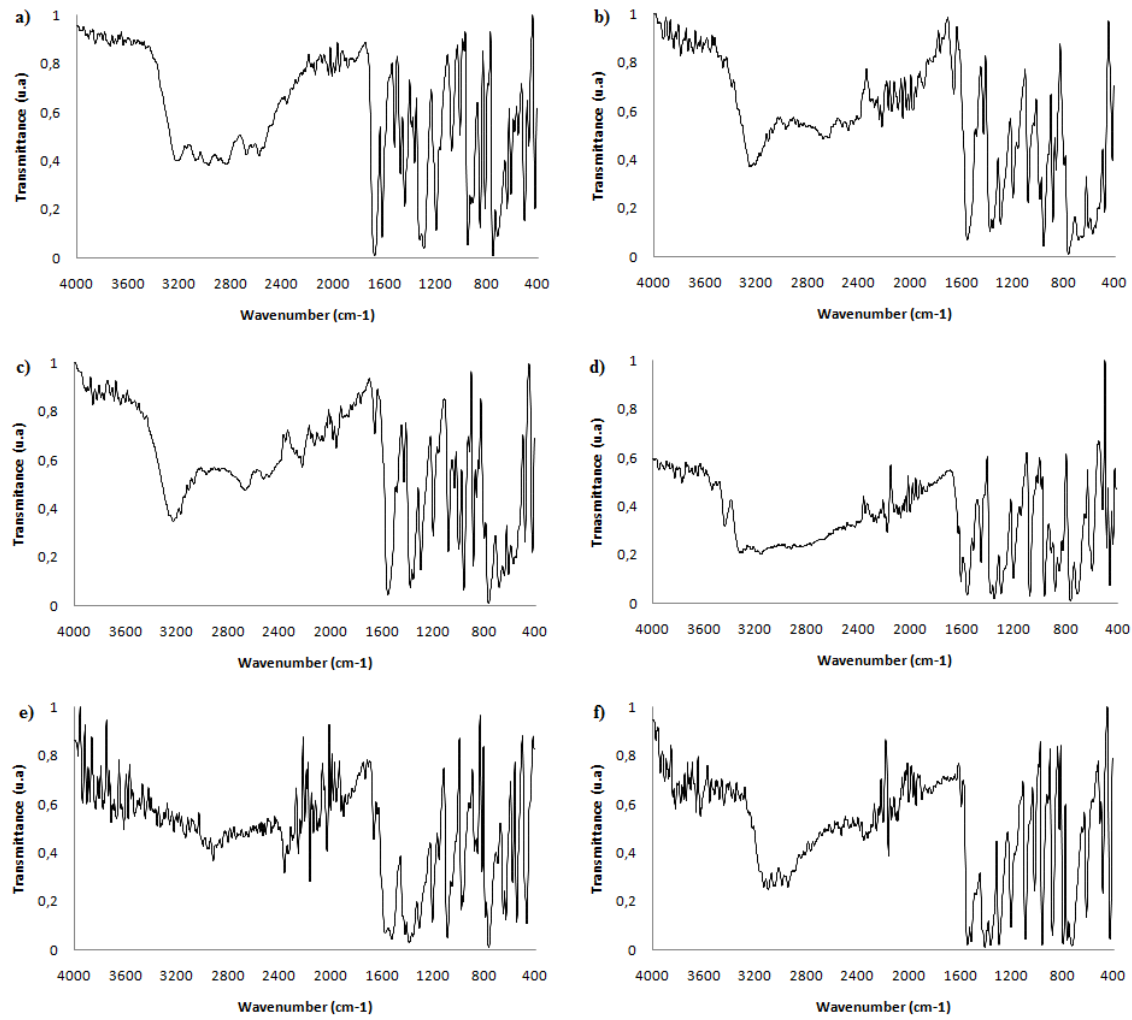


Figure S9. - FTIR spectra of a) Ligand 1H-Indazole-4-carboxylic acid; b) compound **1**; c) compound **2**; d) compound **3**; e) compound **4**; f) compound **5**.